Supplementary

X-ray Diffraction (XRD) analysis:

X-ray diffraction pattern was used to identify the crystal structure of the nanoparticles. The XRD patterns for Fe_3O_4 nanoparticles and CS-Fe_3O_4 are shown in Figure S1. The Fe_3O_4 diffraction patterns have six main peaks at 2θ values of 30.1°, 35.5°, 43.2°, 53.5°, 57°, and 62.8° corresponding to the (220), (311), (400), (422), (511), and (440) crystal planes. Positions and relative intensities of all the peaks are in accordance with cubic spinel system of Fe_3O_4 nanoparticles. The narrow shape peaks of Fe_3O_4 indicate that the nanoparticles have relatively high crystallinity. In the XRD pattern of as prepared Fe_3O_4-chitosan hybrid nanoparticles, a broad peak was observed at around 2 theta (2θ) = 22.6°, which was corresponding to chitosan[23]. Meanwhile, two diffraction peaks were also observed at 2θ = 35.6°and 62.8°, corresponding to (311) and (440) crystal planes of Fe_3O_4, respectively.

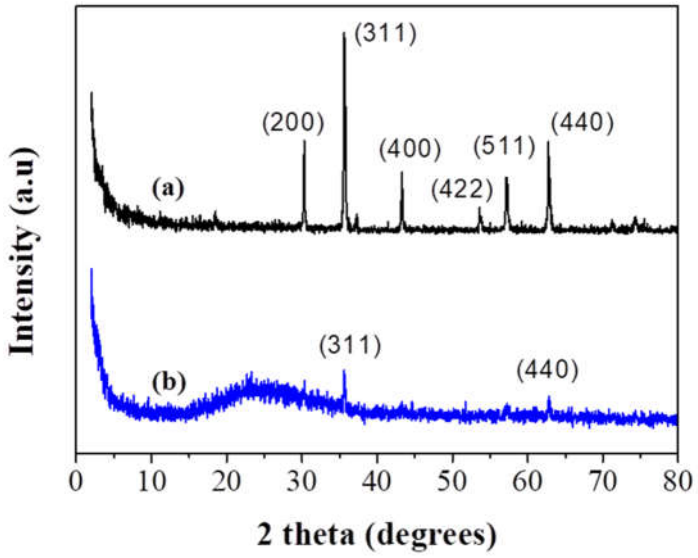

Figure S1: X-ray Powder Diffraction (XRPD) patterns of (a) Fe_3O_4 and (b) Fe_3O_4 chitosan nanoparticles.

Table S1: Concentration of the released hydroxytyrosol through the hydrolysis of oleuropein from lipases of different origin (the standard deviation was less than 5% in all cases).

Enzyme	Hydroxytyrosol (mg mL^{-1})
Lipase A from *Candida antarctica* (CalA)	0.9
Lipase B from *Candida antarctica* (CalB)	0.2
Lipase from *Thermomyces lanuginosus*	0.3
Lipase from *Aspergillus oryzae*	0.1
Lipase from *Mucor miehei*	0.1

Table S2: Concentration of the released hydroxytyrosol through the hydrolysis of oleuropein through different combinations of the enzymes bgl and CalA (the standard deviation was less than 5% in all cases).

Sample	Hydroxytyrosol (mg mL^{-1})
Free form of bgl	0.2
Free form of CalA	0.9
Mixture of free bgl and CalA	1.6

Nuclear Magnetic Resonance (NMR) Analysis:

Nuclear magnetic resonance (NMR) was employed for the characterization of the products of the enzymatic hydrolysis of oleuropein, such as hydroxytyrosol, elenolic acid and glucose. In Figure S3 (d) in the ^{1}H-NMR spectra of the reaction mixture the chemical shifts of the aromatic protons (2H, 5H and 6H) of hydroxytyrosol can be seen clearly. The same applies for the protons at the positions C3′, C4′ and the 4′CH_3 protons of elenolic acid, and the 1′H proton of glucose. The rest of the chemicals shifts of the above compounds have been identified in the area between 2 to 4 ppm. No oleuropein have been detected in the reaction mixture confirming the 100% conversion yield of oleuropein.

^{1}H-NMR chemical shifts of:

Hydroxytyrosol: ^{1}H NMR (500 MHz, D_2O): δ 6.80 (d, J = 8.0 Hz, 1H, 6c-H), 6.76 (s, 1H, 2c-H), 6.66 (d, J = 8.0 Hz, 1H, 5c-H), 3.70 (t, J = 6.7 Hz, 2H, 8c-H), 2.66 (t, J= 6.7Hz, 2H, 7c-H);

Oleuropein: ^{1}H NMR (500 MHz, D_2O): δ 7.46 (s, 1H, 3′c-H), 6.82 (d, J = 8.0 Hz, 1H, 6c-H), 6.77 (s, 1H, 2c-H), 6.67 (d, J = 8.0 Hz, 1H, 5c-H), 5.97 (q, J = 7.0 Hz, 2H, 6′c-H), 5.70 (s, 1H, 4′c-H), 4.27 (m, 1H, 6″c-Ha), 4.12 (m, 1H, 6″c-Hb), 3.84 (m, 2H, 8c-H), 3.50 (t, J = 9.0 Hz, 1H, 1′c-H), 3.44 (m, 1H, 1″c-H), 3.38 (m, 2H, 2″c-H, 5″c-H), 2.78 (m, 2H, 3″c-H, 4″c-H), 2.46 (m, 1H, 10c-H), 1.52 (d, J = 7.0 Hz, CH3, 7c-H);

Glucose: ^{1}H NMR (500 MHz, D_2O): δ 5.20 (s, 1H, 1c-H), 3.84 (m, 2H, 2c-H, 5c-H), 3.70 (m, 2H, 3c-H, 4c-H), 3.38 (m, 1H, 6c-Ha), 3.22 (m, 1H, 6c-Hb);

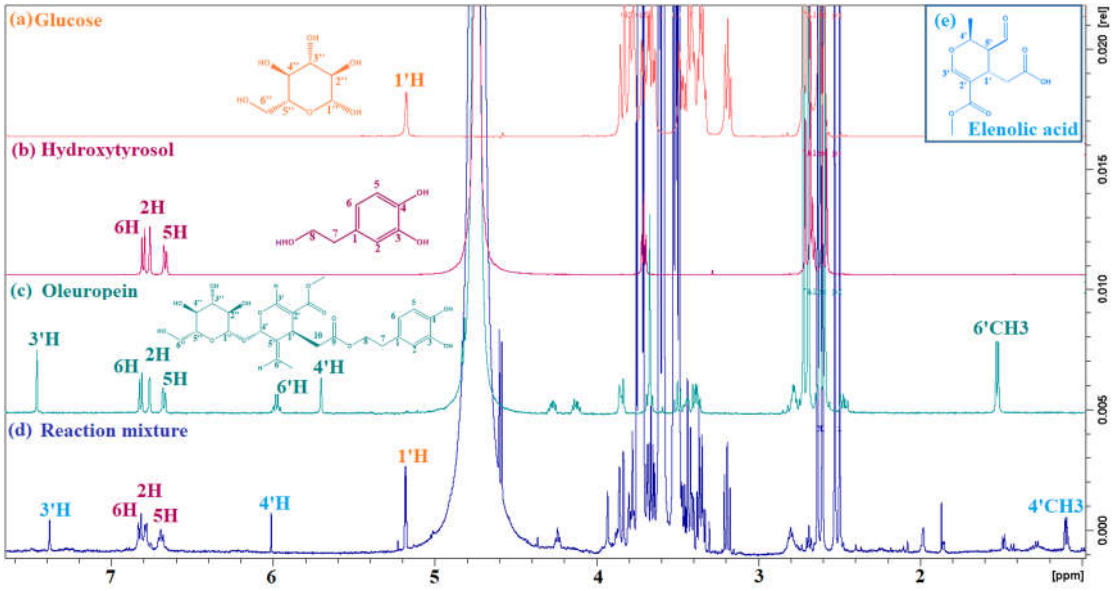

Figure S2. Superposition of ^{1}H-NMR spectra of (a) glucose, (b) hydroxytyrosol, (c) oleuropein and (d) the reaction mixture of the enzymatic hydrolysis of oleuropein by the bi-enzymatic nanobiocatalytic system of co-immobilized bgl-CalA, in citrate-phosphate buffer 100 mM, pH 6.5 in D_2O. In the inset (e) the structure of elenolic acid is illustrated.

Figure S3. Magnetic separation of the CS MNPs.